Nonlinear Waves in Two-Dimensional Autonomous Cellular Neural Networks Coupled by Memristors

Makoto Itoh[1]
1-19-20-203, Arae, Jonan-ku,
Fukuoka, 814-0101 JAPAN
Email: itoh-makoto@jcom.home.ne.jp

Abstract
In this paper, we propose two-dimensional autonomous cellular neural networks (CNNs), which are formed by connecting single synaptic-input CNN cells to each node of an *ideal memristor grid*. Our computer simulations show that the proposed two-dimensional autonomous CNNs can exhibit interesting and complex nonlinear waves. In some autonomous CNNs, we have to choose a *locally active* memristor grid, in order for the autonomous CNNs to exhibit the *continuous evolution* of nonlinear waves. Some other notable features are: The autonomous Van der Poll type CNN can exhibit various kinds of nonlinear waves by changing the *characteristic curve* of the nonlinear resistor in the CNN cell. Furthermore, if we choose a different step size in the numerical integration, it exhibits a different nonlinear wave. The autonomous Lotka-Volterra CNN can also exhibit various kinds of nonlinear waves by changing the *initial conditions*. That is, it can exhibit different response for each initial condition. Furthermore, we have to choose a *passive* memristor grid to avoid an *overflow* in the numerical integration process of this CNN. Our computer simulations show that the dynamics of the proposed autonomous CNNs are more complex than we expected.

Keywords
memristor; CNN; complex nonlinear waves; two-dimensional array; memristor grid; Lotka-Volterra equations; Rössler equations; Brusselator equations; Gierer-Meinhardt equations; Tyson-Kauffman equations; Van der Pol oscillator; FitzHugh-Nagumo equations; Chua circuit; Hamilton's equations.

1 Introduction

The memristor cellular neural network (memristor CNN)[2] has the suspend and resume feature, and it has the functions of the short-term and long-term memories. It can also exhibit many interesting two-dimensional waves by adding an inductor to each CNN cell [1]. In this paper, we propose two-dimensional *autonomous* (i.e., having no inputs) CNNs, which are formed by connecting single synaptic-input CNN cells to each node of an ideal memristor grid. The CNN cells can be realized by the three element memristor circuits in [2] or the nonlinear circuits in [3, 4]. The two-dimensional autonomous CNNs are defined by large nonlinear systems of first-order ordinary differential equations. Thus, we use the simple Euler method to find the solutions of the autonomous CNNs, which is the most basic method for numerical integration. Furthermore, we assume the *Neumann* (zero-flux) boundary condition. It means that there is no current flow from the

[1]After retirement from Fukuoka Institute of Technology, he has continued to study the nonlinear dynamics on memristors.
[2]The terminology CNN was originally used for Cellular Neural Network [5, 6]. Recently, CNN is also used for Convolutional Neural Network. In this paper, CNN stands for Cellular Neural Network.

boundary in the border cells, that is, the boundary does not affect the dynamics of the two-dimensional autonomous CNNs.

Our computer simulations show that the proposed two-dimensional autonomous CNNs can exhibit interesting and complex nonlinear waves, as shown in Fig. 1. In some autonomous CNNs, we have to choose a *locally active* memristor grid, in order for the autonomous CNNs to exhibit the *continuous evolution* of nonlinear waves. Some other notable features are: The autonomous Van der Poll type CNN can exhibit various kinds of nonlinear waves by changing the *characteristic curve* of the nonlinear resistor in the CNN cell. Furthermore, if we choose a different step size in the numerical integration, it exhibits a different nonlinear wave. The autonomous Lotka-Volterra CNN can also exhibit various kinds of nonlinear waves by changing the *initial conditions*. That is, it can exhibit different response for each initial condition. Furthermore, we have to choose a *passive* memristor grid to avoid an *overflow* in the numerical integration process of this CNN. Our computer simulations show that the dynamics of the proposed autonomous CNNs are more complex than we expected.

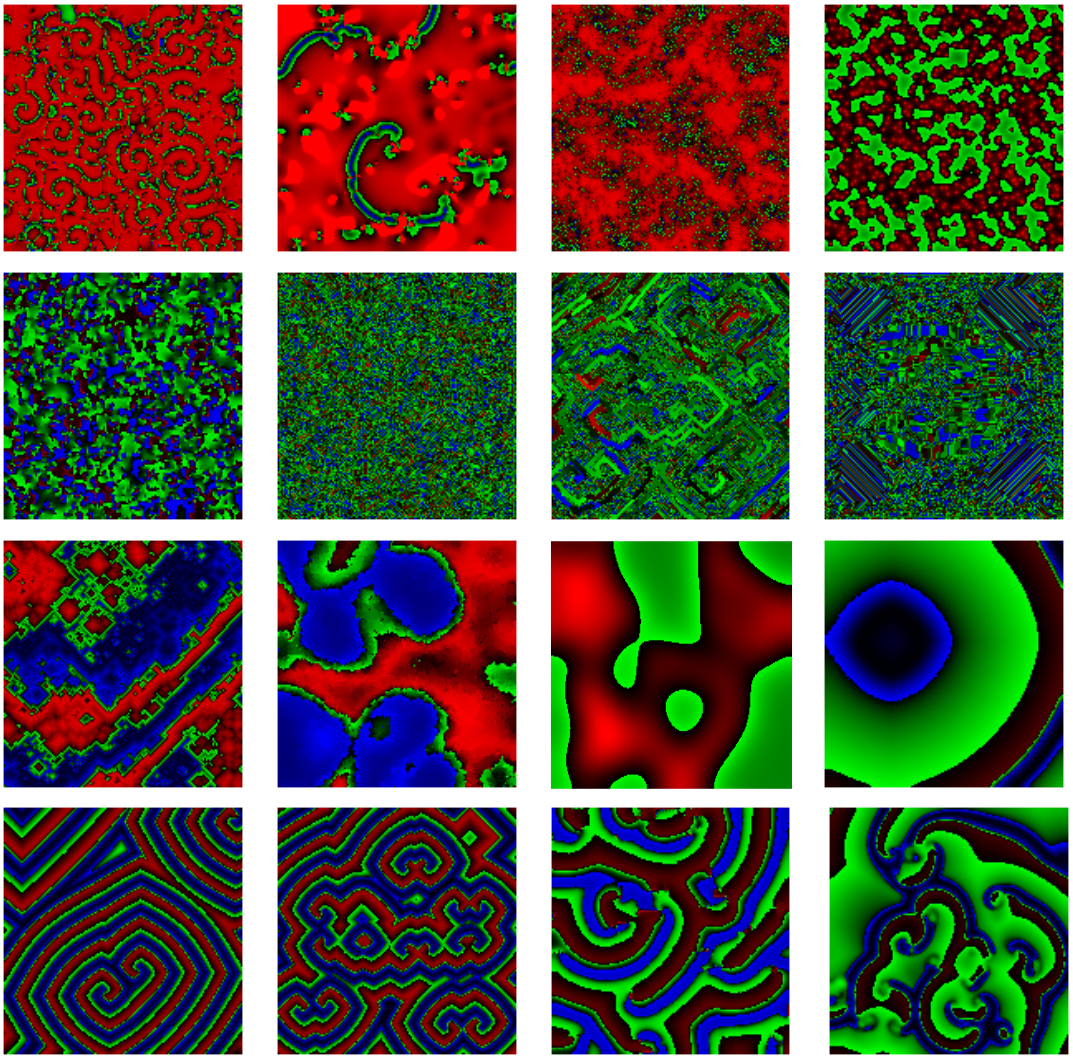

Figure 1: Nonlinear waves in the two-dimensional autonomous CNN. These figures are not static, but dynamic (always changing) images at an instant.

2 Two-Dimensional Autonomous Brusselator CNN

Consider the two-dimensional *autonomous* CNNs containing $N \times N$ cells shown in Fig. 2, which are formed by connecting *single synaptic-input CNN cells* (colored in red) to each node of a *voltage-controlled ideal memristor grid* (colored in peach and navy).

As stated in Sec. 1, we can use the memristor circuits, or the nonlinear circuits in [3, 4], as the single synaptic-input CNN cells. In the case of the memristor circuits, we have to use the three element memristor circuit shown in Fig. 3, since the grid consists of voltage-controlled ideal memristors. Note that the memristor circuit in Fig. 3 is the *dual* of the circuit given in [2]. That is, these two circuits have identical dynamics (see [7] for more details).

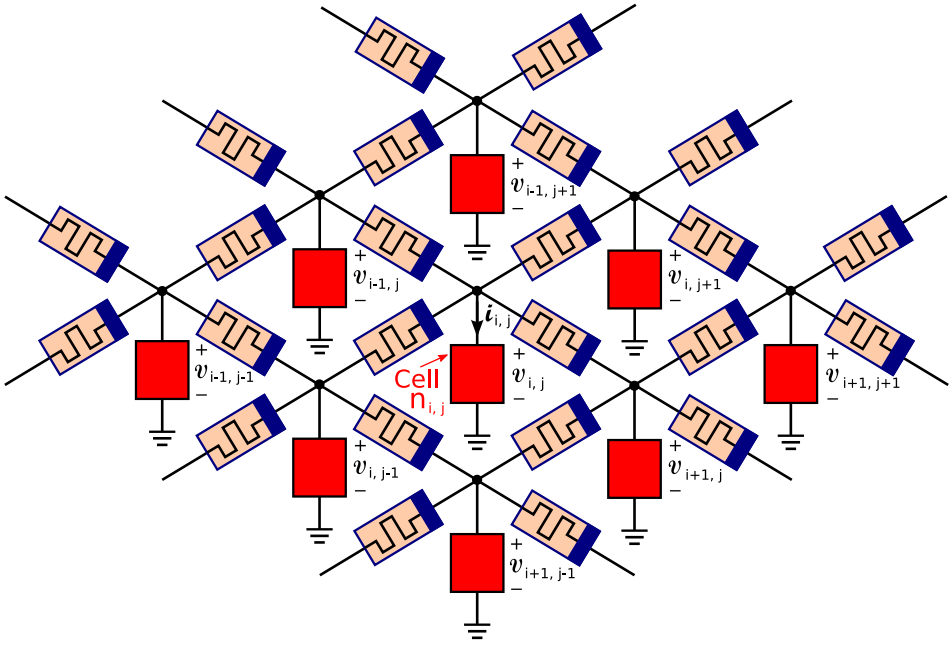

Figure 2: Two-dimensional autonomous CNN formed by connecting single synaptic-input CNN cells (colored in red) to each node of a nonlinear voltage-controlled ideal memristor grid (colored in peach and navy), where $v_{i,j}$ indicates the voltage across the CNN cell $n_{i,j}$ and $i_{i,j}$ indicates the current though the CNN cell $n_{i,j}$.

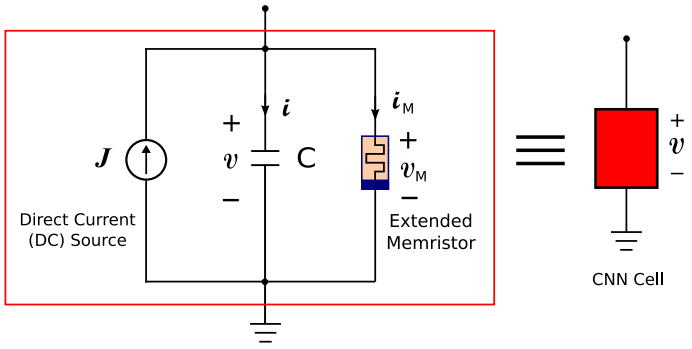

Figure 3: Memristor circuit realization of a single synaptic-input CNN cell. It consists of a linear capacitor C, a direct current source J, and a voltage-controlled extended memristor defined by Eq. (1).

The terminal voltage v_M and the terminal current i_M of the voltage-controlled *extended* memristor in Fig. 3 are described by

$$\left.\begin{array}{rcl} i_M &=& \hat{G}(\boldsymbol{x},\ v_M)\, v_M, \\ \dfrac{d\boldsymbol{x}}{dt} &=& \tilde{\boldsymbol{g}}(\boldsymbol{x},\ v_M), \end{array}\right\} \tag{1}$$

where $\boldsymbol{x} = (x_1,\, x_2,\, \cdots,\, x_n) \in \mathbb{R}^n$ are the state variables of the extended memristor, $\hat{G}(\boldsymbol{x},\ v_M)$ is a continuous scalar-valued function satisfying $\hat{G}(\boldsymbol{x},\ 0) \neq \infty$, and $\tilde{\boldsymbol{g}} = (\tilde{g}_1,\, \tilde{g}_2,\, \cdots,\, \tilde{g}_n) : \mathbb{R}^n \to \mathbb{R}^n$.[3] Thus the dynamics of the three-element memristor circuit (CNN cell) in Fig. 3 is given by

$$\left.\begin{array}{rcl} C\dfrac{dv}{dt} &=& -i_M + J = -\hat{G}(\boldsymbol{x},\ v)\, v + J, \\ \dfrac{d\boldsymbol{x}}{dt} &=& \tilde{\boldsymbol{g}}(\boldsymbol{x},\ v), \end{array}\right\} \tag{2}$$

where C denotes the capacitance of the linear capacitor, J denotes the current of DC (direct current) source, and $v_M = v$.

(1) Brusselator equations

Assume that Eq. (2) satisfies

$$\left.\begin{array}{rcc} C &=& 1, \\ J &=& A, \\ \hat{G}(x,\, v) &=& -\big\{v\, x - (B+1)\big\}, \\ \tilde{g}_1(x, v) &=& Bv - v^2\, x, \end{array}\right\} \tag{3}$$

where $A = 1$, $B = 3$, $\boldsymbol{x} = x \in \mathbb{R}$ is the state variable of the *extended* memristor, $\hat{G}(\boldsymbol{x},\ v) = \hat{G}(x,\, v)$, and $\tilde{\boldsymbol{g}}(\boldsymbol{x},\ v) = \tilde{g}_1(x,\ v)$. Then, Eqs. (1) and (2) can respectively be recast into the forms

$$\left.\begin{array}{rcl} i_M &=& -\big\{v_M\, x - (B+1)\big\}v_M, \\ \dfrac{dx}{dt} &=& B\, v_M - {v_M}^2\ x, \end{array}\right\} \tag{4}$$

and

$$\left.\begin{array}{rcl} \dfrac{dv}{dt} &=& A + \big\{vx - (B+1)\big\}v, \\ \dfrac{dx}{dt} &=& B\, v - v^2\, x, \end{array}\right\} \tag{5}$$

where $A = 1$, $B = 3$, and $v_M = v$. Equations (5) are equivalent to the Brusselator equations (see [2, 4]).

(2) Autonomous Brusselator CNN

In the case of the Brusselator equations (5), the dynamics of the two-dimensional *autonomous* CNN in Fig. 2 is described by

$$\left.\begin{array}{rcl} \dfrac{dv_{i,j}}{dt} &=& A + \big\{v_{i,j}x_{i,j} - (B+1)\big\}v_{i,j} + i_{i,j}, \\ \dfrac{dx_{i,j}}{dt} &=& B\, v_{i,j} - {v_{i,j}}^2\, x_{i,j}, \\ \dfrac{d\varphi_{i,j}}{dt} &=& v_{i,j}, \end{array}\right\} \tag{6}$$

[3] We used the same symbols given in Appendix A of [2]. See [8] for more details on the voltage-controlled extended memristor.

where $A = 1$, $B = 3$, $i = 1, 2, \cdots, N$, $j = 1, 2, \cdots, M$, and the four state variables: $v_{i,j}$, $i_{i,j}$, $x_{i,j}$, and $\varphi_{i,j}$ of the CNN cell $n_{i,j}$ are explained as follow:

- $v_{i,j}$ is the voltage across the CNN cell, that is, the voltage across the capacitor C in the CNN cell.
- $i_{i,j}$ is the current though the CNN cell.
- $x_{i,j}$ is the state variable of the voltage-controlled *extended* memristor (see Eqs. (1) and (4)).
- $\varphi_{i,j}$ is the flux of the capacitor C in the CNN cell.

The current $i_{i,j}$ in Eq. (6) is given by

$$\begin{aligned} i_{i,j} &= i_1 - i_2 + i_3 - i_4 \\ &= W_g(\varphi_{i-1,j} - \varphi_{i,j})(v_{i-1,j} - v_{i,j}) - W_g(\varphi_{i,j} - \varphi_{i+1,j})(v_{i,j} - v_{i+1,j}) \\ &\quad + W_g(\varphi_{i,j-1} - \varphi_{i,j})(v_{i,j-1} - v_{i,j}) - W_g(\varphi_{i,j} - \varphi_{i,j+1})(v_{i,j} - v_{i,j+1}), \end{aligned} \tag{7}$$

where i_1, i_2, i_3 and i_4 are the current through the voltage-controlled *ideal* memristors consisting the grid (see Fig. 4). They are given by

$$\left.\begin{aligned} i_1 &= W_g(\varphi_{i-1,j} - \varphi_{i,j})(v_{i-1,j} - v_{i,j}), \\ i_2 &= W_g(\varphi_{i,j} - \varphi_{i+1,j})(v_{i,j} - v_{i+1,j}), \\ i_3 &= W_g(\varphi_{i,j-1} - \varphi_{i,j})(v_{i,j-1} - v_{i,j}), \\ i_4 &= W_g(\varphi_{i,j} - \varphi_{i,j+1})(v_{i,j} - v_{i,j+1}), \end{aligned}\right\} \tag{8}$$

where $W_g(\varphi_g)$ denotes the small-signal memductance of the voltage-controlled ideal memristors consisting the grid. Their terminal current i_g and voltage v_g are described by

$$i_g = W_g(\varphi_g)\, v_g, \tag{9}$$

where φ_g is the flux of the ideal memristor, which satisfies $\dfrac{d\varphi_g}{dt} = v_g$ and we assume that $\varphi_g(0) = 0$.

If we replace the ideal memristor grid with the *linear resistor* grid, then we obtain the two-dimensional *reaction-difusins* CNN described in [4]. In this case, Eqs. (6) and (7) can respectively be recast into the forms

$$\left.\begin{aligned} \frac{dv_{i,j}}{dt} &= A + \big\{v_{i,j}x_{i,j} - (B+1)\big\}v_{i,j} + i_{i,j}, \\ \frac{dx_{i,j}}{dt} &= B\, v_{i,j} - {v_{i,j}}^2\, x_{i,j}, \end{aligned}\right\} \tag{10}$$

and

$$i_{i,j} = D\,(v_{i-1,j} + v_{i+1,j} + v_{i,j-1} + v_{i,j+1} - 4v_{i,j}), \tag{11}$$

where D is a conductance of the linear resistors consisting the grid, $i = 1, 2, \cdots, N$, and $j = 1, 2, \cdots, M$. Note that Eq. (10) becomes a *lower* dimensional system, since the third equation in Eq. (6) disappears.

(3) Boundary condition

In this paper, we apply the zero-flux (Neumann) boundary condition to the two-dimensional *autonomous* CNN (6):

$$\left.\begin{aligned} v_{i,0} &\triangleq v_{i,0} = v_{i,1}, & i &= 1, 2, \cdots, N \\ v_{i,N+1} &\triangleq v_{i,N+1} = v_{i,N}, & i &= 1, 2, \cdots, N \\ v_{0,j} &\triangleq v_{0,j} = v_{1,j}, & j &= 1, 2, \cdots, M \\ v_{N+1,j} &\triangleq v_{N+1,j} = v_{N,j}, & j &= 1, 2, \cdots, M. \end{aligned}\right\} \tag{12}$$

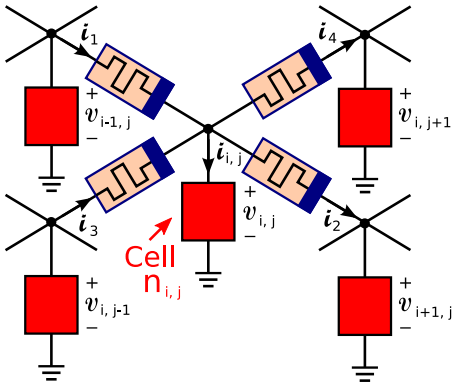

Figure 4: Currents through the voltage-controlled ideal memristors: i_1, i_2, i_3 and i_4.

Thus, there is no current flow from the boundary in the border cells, that is, the boundary does not affect the dynamics of the two-dimensional autonomous CNN (6).

(4) Memristors in the grid

Consider the state equations of the two-dimensional autonomous Brusselator CNN, which is given by Eq. (6). Assume that the terminal current i_g and voltage v_g of the voltage-controlled *ideal* memristors in the grid are described by by

$$\left.\begin{array}{rcl} i_g & = & W_g(\varphi_g)\, v_g, \\ \dfrac{d\varphi_g}{dt} & = & v_g, \end{array}\right\} \tag{13}$$

where $W_g(\varphi_g)$ is the small-signal memductance of the voltage-controlled ideal memristors, which is shown in Fig. 5. It is given by a piecewise linear function of the form:

$$\left.\begin{array}{rcl} W_g(\varphi_g) & = & -0.25\,\mathfrak{s}\big[\,|\,\varphi_g\,|-0.5\,\big]+0.5\,\mathfrak{s}\big[\,|\,\varphi_g\,|-10\,\big] \\ & = & \left\{\begin{array}{rcl} 0 & \text{for} & |\varphi_g|<0.5, \\ -0.25 & \text{for} & 0.5\le|\varphi_g|<10, \\ 0.25 & \text{for} & |\varphi_g|\ge 10, \end{array}\right. \end{array}\right\} \tag{14}$$

where $\mathfrak{s}[\,z\,]$ denotes the *unit step* function, which is equal to 0 for $z<0$ and 1 for $z\ge 0$. Compare Eq. (13) with Eq. (1).

Assume that $0.5<|\varphi_g(t)|<10$ and $v_g(t)\neq 0$. Then $W_g(\varphi_g)=-0.25<0$, and the *instantaneous* power $p(t)$ of the voltage-controlled ideal memristors in the grid satisfies

$$p(t)=i_g(t)\,v_g(t)=\big(W_g(\varphi_g(t))\,v_g(t)\big)\,v_g(t)=W_g(\varphi_g(t))\,v_g(t)^2=-0.25v_g(t)^2<0. \tag{15}$$

Thus, these memristors are *locally active*.[4]

(5) Behavior of the memristors in the grid

In the autonomous Brusselator CNN (6), individual cells are disconnected from their neighbors at first, that is, they independently operate without interaction. It is due to the reason that the current $i_{i,j}(t)$ in Eq. (7) is equal to zero, if $|\varphi_{i,j}|$ is sufficiently small.

[4]In the Oregonator CNN model [9], the *monotonically increasing* function $W_g(\varphi_g)$ is used to generate spiral patterns. In this paper, we used $W_g(\varphi_g)$ defined by Eq. (14), since the initial conditions are different from those of [9].

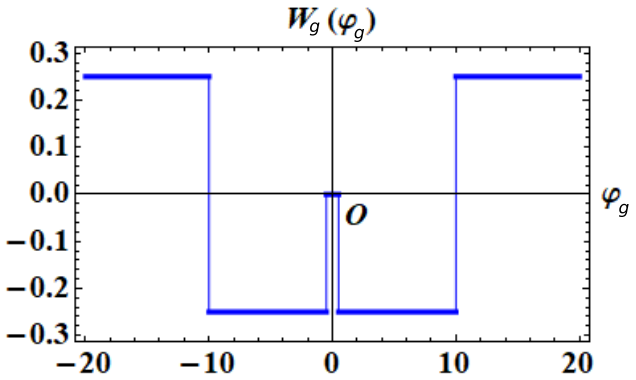

Figure 5: Memductance $W_g(\varphi_g)$ of the ideal memristor, which is given by a piecewise linear function of the form $W_g(\varphi_g) = 0.25\,\mathfrak{s}\big[\,|\,\varphi_g\,|-0.5\,\big] + 0.5\,\mathfrak{s}\big[\,|\,\varphi_g\,|-10\,\big]$. Note that $W_g(\varphi_g) = 0$ for $|\varphi_g| < 0.5$.

Let us explain its details. Define $\varphi^{\dagger} \in \big\{\,(\varphi_{i-1,j} - \varphi_{i,j}),\, (\varphi_{i,j} - \varphi_{i+1,j}),\, (\varphi_{i,j-1} - \varphi_{i,j}),\, (\varphi_{i,j} - \varphi_{i,j+1})\,\big\}$, where $i = 1, 2, \cdots, N$, $j = 1, 2, \cdots, M$. Assume that $\varphi_{i,j}(0) = 0$. Then $\varphi^{\dagger}(0) = 0$. Assume next that the time t is sufficiently small. Then we obtain $W_g(\varphi^{\dagger}(t)) = 0$, since $|\varphi^{\dagger}(t)| < 0.5$ for $0 \le t \ll 1$. Thus, the current $i_{i,j}(t)$ given by Eq. (7) is equal to zero, and individual cells are disconnected from their neighbors at first. that is, they independently operate without interaction. However, they interact each other when the current $i_{i,j}$ becomes non-zero by increasing $|\varphi^{\dagger}(t)|$.

(6) Computer simulations

In order to obtain the solutions of the autonomous Brusselator CNN (6), we assume the followings:

1. The initial condition $v_{i,j}(0)$ is given by a black & white image in Fig. 6(1), or a gray-scale image in Fig. 6(2), where the luminance value of the pixel would be coded as black $\to +1$, white $\to -1$, gray $\to (-1,\ 1)$.
2. $x_{i,j}(0) = 0$ and $\varphi_{i,j}(0) = 0$.
3. The boundary condition for the state $v_{i,j}$ is given by Eq. (12).

Then, from our computer simulations, we obtain Fig. 7, which shows the two-dimensional nonlinear waves for the state $v_{i,j}$. Observe that the autonomous Brusselator CNN (6) can exhibit the complex nonlinear waves. Note that in order to view the wave patterns clearly, we coded the state $v_{i,j}$ as follows: the color evolves continuously through red, green, blue, and black as $v_{i,j}$ increases.[5] Furthermore, we used the simple Euler method to find the solutions of the autonomous Brusselator CNN (6).[6]

[5] In some other examples, we also coded the wave patterns in *reverse order*, that is, black, blue, green, and red, since $v_{i,j}(t)$ is oscillating. Furthermore, we used the *nonlinear* color curve to emphasize the wave patterns (by increasing or decreasing the intensity of the individual color).

[6] If the image size of the initial condition is $N \times M = 145 \times 150$, then we have to solve a system of $3 \times N \times M = 3 \times 145 \times 150 = 65250$ first-order differential equations. Thus, we used the simple Euler method for solving Eq. (6). It is the most basic method for numerical integration. We can write the Euler Method for Eq. (6) as follow:

$$\left.\begin{aligned} v_{i,j}(t+h) &= h\,\big[\,A + \{v_{i,j}(t)x_{i,j}(t) - (B+1)\}v_{i,j}(t) + i_{i,j}(t)\,\big] + v_{i,j}(t), \\ x_{i,j}(t+h) &= h\,\big[\,B\,v_{i,j}(t) - v_{i,j}(t)^2\,x_{i,j}(t)\,\big] + x_{i,j}(t), \\ \varphi_{i,j}(t+h) &= h\,v_{i,j}(t) + \varphi_{i,j}(t), \end{aligned}\right\} \tag{16}$$

where h denotes the step size for the numerical integration and it is reasonably small. By repeating the above process, we can get $\{v_{i,j}(t+h),\, x_{i,j}(t+h),\, \varphi_{i,j}(t+h)\}$, $\{v_{i,j}(t+2h),\, x_{i,j}(t+2h),\, \varphi_{i,j}(t+2h)\}$, $\cdots$, $\{v_{i,j}(t+nh),\, x_{i,j}(t+nh),\, \varphi_{i,j}(t+nh)\}$, where n is an integer. Thus, the Euler method advances a solution through an interval h using derivative information. This

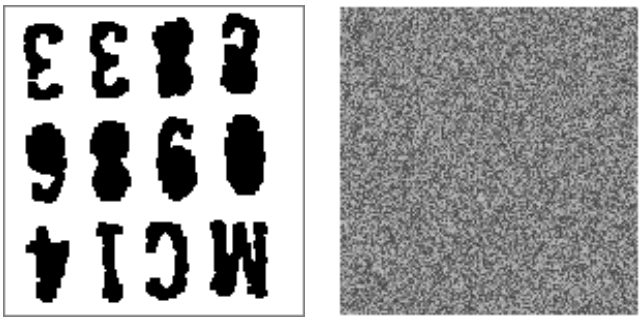

(1) upside-down text (2) random noise

Figure 6: Two images for the initial condition $v_{i,j}(0)$. They are both 145×150 pixels in size. (1) a black & white upside-down text image. (2) a gray-scale random noise image.

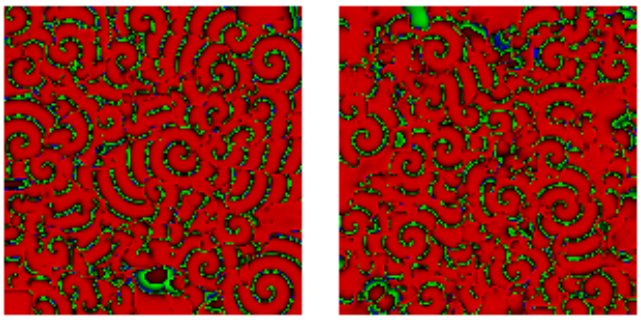

(a) $t = 4000$ (b) $t = 4000$

Figure 7: Two-dimensional nonlinear waves in the autonomous Brusselator CNN (6). These figures are not static, but dynamic (always changing) images at the instant of $t = 4000$. (a) The initial condition $v_{i,j}(0)$ is given by the upside-down text image in Fig. 6(1). The step size h of the Euler method is set to 0.05. (b) The initial condition $v_{i,j}(0)$ is given by the random noise image in Fig. 6(2). The step size h of the Euler method is set to 0.04.

method may be neither accurate nor stable, however, it is attractive because of its simplicity. When $h = 1$, Eq. (16) is considered to be a discrete-time cellular neural network (DTCNN).

3 Examples of Two-Dimensional Nonlinear Waves

In this section, we show several examples of two-dimensional autonomous CNNs and their waves.

3.1 Autonomous Gierer-Meinhardt CNN

The *diffusion-less* and *time-scaled* Gierer-Meinhardt equations are described by (see [2] for more details)

$$\left.\begin{aligned} \frac{dv}{dt} &= (v - b\,x)\,v, \\ \frac{dx}{dt} &= e\,(v^2 - c\,x)\,x, \end{aligned}\right\} \tag{17}$$

where $b = 0.65$, $c = 0.796$, and $e = 0.2$.[7] Equation (17) can be realized by the three-element memristor circuit in Fig. 3. Assume that Eq. (2) satisfies

$$\left.\begin{aligned} C &= 1, \\ J &= 0, \\ \hat{G}(x,\,v) &= -(v - b\,x)\,v, \\ \tilde{g}_1(x,v) &= e\,(v^2 - c\,x)\,x, \end{aligned}\right\} \tag{18}$$

where $\boldsymbol{x} = x \in \mathbb{R}$ is the state variable of the extended memristor, $\hat{G}(\boldsymbol{x},\,v) = \hat{G}(x,\,v)$, and $\tilde{\boldsymbol{g}}(\boldsymbol{x},\,v) = \tilde{g}_1(x,\,v)$. Then Eq. (2) can be recast into Eq. (17).

In this case, the dynamics of the two-dimensional autonomous CNN in Fig. 2 is described by

$$\left.\begin{aligned} \frac{dv_{i,j}}{dt} &= (v_{i,j} - b\,x_{i,j})v_{i,j} + i_{i,j},, \\ \frac{dx_{i,j}}{dt} &= e\,({v_{i,j}}^2 - c\,x_{i,j})x_{i,j}, \\ \frac{d\varphi_{i,j}}{dt} &= v_{i,j}, \end{aligned}\right\} \tag{19}$$

where $i = 1, 2, \cdots, N$, $j = 1, 2, \cdots, M$, and the four state variables of the CNN cell $n_{i,j}$ are explained as follow:

- $v_{i,j}$ is the voltage across the CNN cell $n_{i,j}$, that is, the voltage across the capacitor C in the CNN cell.
- $i_{i,j}$ is the current though the CNN cell.
- $x_{i,j}$ is the state variable of the voltage-controlled *extended* memristor in the CNN cell (see Eq. (1)).
- $\varphi_{i,j}$ is the flux of the capacitor C in the CNN cell.

The current $i_{i,j}$ in Eq. (19) is given by

$$\begin{aligned} i_{i,j} \;=\; & W_g(\varphi_{i-1,j} - \varphi_{i,j})(v_{i-1,j} - v_{i,j}) - W_g(\varphi_{i,j} - \varphi_{i+1,j})(v_{i,j} - v_{i+1,j}) \\ & + W_g(\varphi_{i,j-1} - \varphi_{i,j})(v_{i,j-1} - v_{i,j}) - W_g(\varphi_{i,j} - \varphi_{i,j+1})(v_{i,j} - v_{i,j+1}), \end{aligned} \tag{20}$$

where $W_g(\varphi_g)$ denotes the small-signal memductance of the voltage-controlled *ideal* memristors consisting the grid. The terminal current i_g and voltage v_g of the above memristors are given by

$$i_g = W_g(\varphi_g)\,v_g, \tag{21}$$

[7] If we change the variables and the parameters: $v \longrightarrow \tilde{v}/e$, $x \longrightarrow \tilde{x}$, $t \longrightarrow e\tau$, $b \longrightarrow \tilde{b}/e$, $c \longrightarrow \tilde{c}/e^2$, then Eq. (17) can be recast into the form

$$\left.\begin{aligned} \frac{d\tilde{v}}{d\tau} &= (\tilde{v} - \tilde{b}\,\tilde{x})\,\tilde{v}, \\ \frac{d\tilde{x}}{d\tau} &= (\tilde{v}^2 - \tilde{c}\,\tilde{x})\,\tilde{x}, \end{aligned}\right\}$$

which is equivalent to the *diffusion-less* and *time-scaled* Gierer-Meinhardt equations in [2].

where φ_g is the flux of the ideal memristor, which satisfies $\dfrac{d\varphi_g}{dt} = v_g$ and $\varphi_g(0) = 0$. Assume that $W_g(\varphi_g)$ is given by

$$\left.\begin{array}{rcl} W_g(\varphi_g) & = & -6\,\mathfrak{s}\big[\,|\,\varphi_g\,| - 0.5\,\big] + 10\,\mathfrak{s}\big[\,|\,\varphi_g\,| - 10\,\big] \\ & = & \left\{\begin{array}{rcl} 0 & \text{for} & |\varphi_g| < 0.5, \\ -6 & \text{for} & 0.5 \le |\varphi_g| < 10, \\ 4 & \text{for} & |\varphi_g| \ge 10. \end{array}\right. \end{array}\right\} \tag{22}$$

Then the ideal memristors consisting the grid are *locally active*, since the instantaneous power $p(t)$ satisfies

$$p(t) = i_g(t)\,v_g(t) = W_g(\varphi_g(t))\,v_g(t)^2 = -6\,v_g(t)^2 < 0, \tag{23}$$

for $0.5 < |\varphi_g(t)| < 10$ and $v_g(t) \neq 0$.

We show the two-dimensional nonlinear waves for $v_{i,j}$ in Fig. 8. Observe that the two-dimensional autonomous Gierer-Meinhardt CNN (19) can exhibit the complex nonlinear waves after very long transient time. Here, the initial conditions $v^*_{i,j}(0)$ and $x^*_{i,j}(0)$ are equal to a black & white image in Fig. 6(1) or a gray-scale image in Fig. 6(2), where $v^*_{i,j}(0)$ and $x^*_{i,j}(0)$ are defined by $v^*_{i,j}(0) = v_{i,j}(0) - 1.1$ and $x^*_{i,j}(0) = x_{i,j}(0) - 1.1$,[8] and we set $\varphi_{i,j}(0) = 0$. The boundary condition is given by Eq. (12).

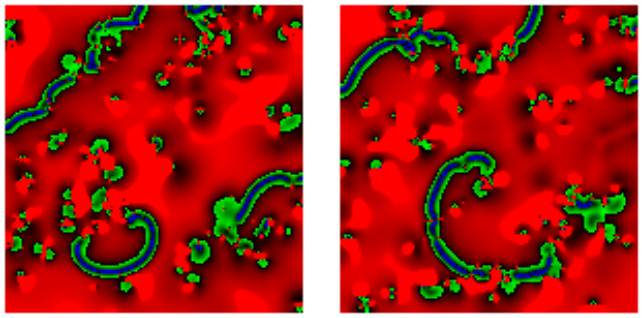

(a) $t = 30000$ (b) $t = 30000$

Figure 8: Two-dimensional nonlinear waves in the autonomous Gierer-Meinhardt CNN (19). These figures are not static, but dynamic (always changing) images at the instant of $t = 30000$. (a) The initial condition $v^*_{i,j}(0)$ is given by the upside-down text image in Fig. 6(1). (b) The initial condition $v^*_{i,j}(0)$ is given by the random noise image in Fig. 6(2). Here, $v^*_{i,j}(0)$ is defined by $v^*_{i,j}(0) = v_{i,j}(0) - 1.1$. The step size h of the Euler method is both set to 0.001.

3.2 Autonomous Tyson-Kauffman CNN

The Tyson-Kauffman equations are described by (see [2] for more details)

$$\left.\begin{array}{rcl} \dfrac{dv}{dt} & = & \alpha\left\{A - (B + D\,x^2)\,v\right\}, \\ \dfrac{dx}{dt} & = & (B + D\,x^2)\,v - d\,x, \end{array}\right\} \tag{24}$$

[8] We shifted the initial conditions in order to avoid an overflow in the numerical simulations.

where $\alpha = 8$, $A = 0.2$, $B = 0.00803$, $D = 1$, and $d = 1$.[9] Equation (24) can be realized by the three-element memristor circuit in Fig. 3. Assume that Eq. (2) satisfies

$$\left.\begin{array}{rcl} C & = & \dfrac{1}{\alpha}, \\ J & = & A, \\ \hat{G}(x,\, v) & = & (B + x^2), \\ \tilde{g}_1(x, v) & = & v + v\, x^2 - x, \end{array}\right\} \tag{25}$$

where $\boldsymbol{x} = x \in \mathbb{R}$ is the state variable of the extended memristor, $\hat{G}(\boldsymbol{x},\, v) = \hat{G}(x,\, v)$, and $\tilde{\boldsymbol{g}}(\boldsymbol{x},\, v) = \tilde{g}_1(x,\, v)$. Then Eq. (2) can be recast into Eq. (24).

In this case, the dynamics of the two-dimensional autonomous CNN in Fig. 2 is described by

$$\left.\begin{array}{rcl} \dfrac{dv_{i,j}}{dt} & = & \alpha \left\{ A - (B + {x_{i,j}}^2)\, v_{i,j} + i_{i,j} \right\}, \\ \dfrac{dx_{i,j}}{dt} & = & (B + {x_{i,j}}^2)\, v_{i,j} - x_{i,j}, \\ \dfrac{d\varphi_{i,j}}{dt} & = & v_{i,j}, \end{array}\right\} \tag{26}$$

where $i = 1, 2, \cdots, N$, $j = 1, 2, \cdots, M$, and the four state variables of the CNN cell $n_{i,j}$ are explained as follow:

- $v_{i,j}$ is the voltage across the CNN cell, that is, the voltage across the capacitor C in the CNN cell.
- $i_{i,j}$ is the current though the CNN cell.
- $x_{i,j}$ is the state variable of the voltage-controlled *extended* memristor (see Eq. (1)).
- $\varphi_{i,j}$ is the flux of the capacitor C.

The current $i_{i,j}$ in Eq. (26) is given by

$$\begin{array}{rcl} i_{i,j} & = & W_g(\varphi_{i-1,j} - \varphi_{i,j})(v_{i-1,j} - v_{i,j}) - W_g(\varphi_{i,j} - \varphi_{i+1,j})(v_{i,j} - v_{i+1,j}) \\ & & + W_g(\varphi_{i,j-1} - \varphi_{i,j})(v_{i,j-1} - v_{i,j}) - W_g(\varphi_{i,j} - \varphi_{i,j+1})(v_{i,j} - v_{i,j+1}), \end{array} \tag{27}$$

where $W_g(\varphi_g)$ denotes the small-signal memductance of the voltage-controlled *ideal* memristors consisting the grid. The terminal current i_g and voltage v_g of the above memristors are given by

$$i_g = W_g(\varphi_g)\, v_g, \tag{28}$$

where φ_g is the flux of the ideal memristor, which satisfies $\dfrac{d\varphi_g}{dt} = v_g$ and $\varphi_g(0) = 0$. Assume that $W_g(\varphi_g)$ is given by

$$\left.\begin{array}{rcl} W_g(\varphi_g) & = & = -\mathfrak{s}\big[\, |\, \varphi_g\, | - 0.5\, \big] + 2\, \mathfrak{s}\big[\, |\, \varphi_g\, | - 7\, \big] \\ & = & \left\{ \begin{array}{cll} 0 & \text{for} & |\varphi_g| < 0.5, \\ -1 & \text{for} & 0.5 \le |\varphi_g| < 7, \\ 1 & \text{for} & |\varphi_g| \ge 7. \end{array} \right. \end{array}\right\} \tag{29}$$

Then the ideal memristors consisting the grid are *locally active*, since the instantaneous power $p(t)$ satisfies

$$p(t) = i_g(t)\, v_g(t) = W_g(\varphi_g(t))\, v_g(t)^2 = -\, v_g(t)^2 < 0, \tag{30}$$

[9] If we change the variables and the parameters: $v \longrightarrow \alpha\tilde{v}$, $x \longrightarrow \tilde{x}, B \longrightarrow \tilde{B}/\alpha$, $D \longrightarrow \tilde{D}/\alpha$, then Eq. (24) can be recast into the form

$$\left.\begin{array}{rcl} \dfrac{d\tilde{v}}{dt} & = & A - (\tilde{B} + \tilde{D}\, \tilde{x}^2)\, \tilde{v}, \\ \dfrac{d\tilde{x}}{dt} & = & (\tilde{B} + \tilde{D}\, \tilde{x}^2) - d\, \tilde{x}, \end{array}\right\}$$

which is equivalent to the Tyson-Kauffman equations in [2].

for $0.5 < |\varphi_g(t)| < 7$ and $v_g(t) \neq 0$.

We show the two-dimensional nonlinear waves for $v_{i,j}$ in Fig. 9. Observe that the autonomous Tyson-Kauffman CNN (26) can exhibit complex nonlinear waves. Here, the initial condition $v_{i,j}(0)$ is equal to a black & white image or a gray-scale image in Fig. 6, and we set $x_{i,j}(0) = \varphi_{i,j}(0) = 0$. The boundary condition is given by Eq. (12).

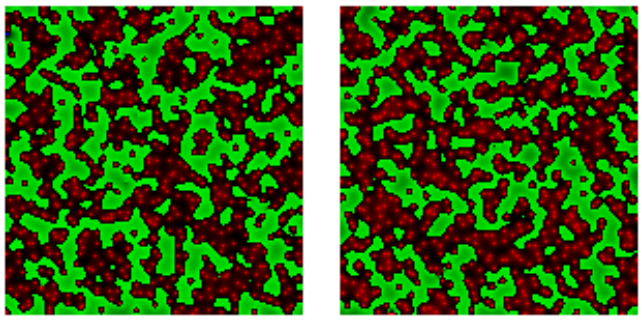

(a) $t = 700$ (b) $t = 700$

Figure 9: Two-dimensional nonlinear waves in the autonomous Tyson-Kauffman CNN (26). These figures are not static, but dynamic (always changing) images at the instant of $t = 700$. (a) The initial condition $v_{i,j}(0)$ is given by the upside-down text image in Fig. 6(1). (b) The initial condition $v_{i,j}(0)$ is given by the random noise image in Fig. 6(2). The step size h of the Euler method is both set to 0.0007.

3.3 Autonomous Rössler CNN

The Rössler equations are described by (see [2] for more details)

$$\left.\begin{aligned} \frac{dv}{dt} &= b + (x - c)\, v, \\ \frac{dx}{dt} &= y + a\, x, \\ \frac{dy}{dt} &= -x - v, \end{aligned}\right\} \tag{31}$$

where $a = 0.1$, $b = 0.1$, and $c = 14$. Equation (31) can be realized by the three-element memristor circuit in Fig. 3. Assume that Eq. (2) satisfies

$$\left.\begin{aligned} C &= 1, \\ J &= b, \\ \hat{G}(x,\, y,\, v) &= -(x - c), \\ \tilde{g}_1(x,\, y, v) &= y + a\, x, \\ \tilde{g}_2(x,\, y, v) &= -x - v, \end{aligned}\right\} \tag{32}$$

where $\boldsymbol{x} = (x,\, y) \in \mathbb{R}^2$ are the state variables of the extended memristor, $\hat{G}(\boldsymbol{x},\ v) = \hat{G}(x, y,\, v)$, and $\tilde{\boldsymbol{g}}(\boldsymbol{x},\ v) = \tilde{\boldsymbol{g}}(x,\, y,\ v) = (\tilde{g}_1(x,\, y,\ v),\ \tilde{g}_2(x,\, y,\ v))$. Then Eq. (2) can be recast into Eq. (31).

In this case, the dynamics of the two-dimensional autonomous CNN in Fig. 2 is described by

$$\left.\begin{array}{rcl} \dfrac{dv_{i,j}}{dt} &=& b + (x_{i,j} - c)\, v_{i,j} + i_{i,j}, \\ \dfrac{dx_{i,j}}{dt} &=& y_{i,j} + a\, x_{i,j}, \\ \dfrac{dy_{i,j}}{dt} &=& -x_{i,j} - v, \\ \dfrac{d\varphi_{i,j}}{dt} &=& v_{i,j}, \end{array}\right\} \tag{33}$$

where $i = 1, 2, \cdots, N$, $j = 1, 2, \cdots, M$, and the five state variables of the CNN cell $n_{i,j}$ are explained as follow:

- $v_{i,j}$ is the voltage across the CNN cell, that is, the voltage across the capacitor C in the CNN cell.
- $i_{i,j}$ is the current though the CNN cell.
- $x_{i,j}$ and $y_{i,j}$ are the state variables of the voltage-controlled *extended* memristor in the CNN cell (see Eqs. (1)).
- $\varphi_{i,j}$ is the flux of the capacitor C in the CNN cell.

The current $i_{i,j}$ in Eq. (33) is given by

$$\begin{array}{rcl} i_{i,j} &=& W_g(\varphi_{i-1,j} - \varphi_{i,j})(v_{i-1,j} - v_{i,j}) - W_g(\varphi_{i,j} - \varphi_{i+1,j})(v_{i,j} - v_{i+1,j}) \\ && + W_g(\varphi_{i,j-1} - \varphi_{i,j})(v_{i,j-1} - v_{i,j}) - W_g(\varphi_{i,j} - \varphi_{i,j+1})(v_{i,j} - v_{i,j+1}), \end{array} \tag{34}$$

where $W_g(\varphi_g)$ denotes the small-signal memductance of the voltage-controlled *ideal* memristors consisting the grid. The terminal current i_g and voltage v_g of the above memristors are given by

$$i_g = W_g(\varphi_g)\, v_g, \tag{35}$$

where φ_g is the flux of the ideal memristor, which satisfies $\dfrac{d\varphi_g}{dt} = v_g$ and $\varphi_g(0) = 0$. Assume that $W_g(\varphi_g)$ is given by

$$\left.\begin{array}{rcl} W_g(\varphi_g) &=& 2\,\mathfrak{s}\big[\,|\,\varphi_g\,| - 0.5\,\big] + \mathfrak{s}\big[\,|\,\varphi_g\,| - 1\,\big] \\ &=& \left\{\begin{array}{lll} 0 & \text{for} & |\varphi_g| < 0.5, \\ 2 & \text{for} & 0.5 \le |\varphi_g| < 1, \\ 3 & \text{for} & |\varphi_g| \ge 1. \end{array}\right. \end{array}\right\} \tag{36}$$

Then the ideal memristors consisting the grid are *passive*, since the instantaneous power $p(t)$ satisfies

$$p(t) = i_g(t)\, v_g(t) = W_g(\varphi_g(t))\, v_g(t)^2 \ge 0. \tag{37}$$

We show the two-dimensional nonlinear waves for $v_{i,j}$ in Fig. 10. The autonomous Rössler CNN (33) can exhibit complex nonlinear waves. Here, the initial conditions $v_{i,j}(0)$, $x_{i,j}(0)$, and $y_{i,j}(0)$ are equal to a black & white image or a gray-scale image in Fig. 6, and we set $\varphi_{i,j}(0) = 0$. The boundary condition is given by Eq. (12).

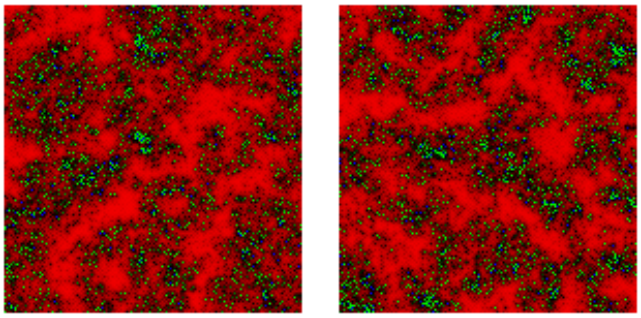

(a) $t = 10000$ (b) $t = 10000$

Figure 10: Two-dimensional nonlinear waves in the autonomous Rössler CNN (33). These figures are not static, but dynamic (always changing) images at the instant of $t = 10000$. (a) The initial condition $v_{i,j}(0)$ is given by the upside-down text image in Fig. 6(1). (b) The initial condition $v_{i,j}(0)$ is given by the random noise image in Fig. 6(2). The step size h of the Euler method is both set to 0.02.

3.4 Autonomous Lotka-Volterra CNN

The Lotka-Volterra equations are described by (see [2] for more details)

$$\left.\begin{array}{rcl} \dfrac{dv}{dt} &=& (c\,x - d)\,v, \\ \dfrac{dx}{dt} &=& (a - b\,v)\,x, \end{array}\right\} \tag{38}$$

where $a = \dfrac{2}{3}$, $b = \dfrac{4}{3}$, and $c = d = 1$. Equation (38) can be realized by the three-element memristor circuit in Fig. 3. Assume that Eq. (2) satisfies

$$\left.\begin{array}{rcl} C &=& 1, \\ J &=& 0, \\ \hat{G}(x,\,v) &=& -(c\,x - d), \\ \tilde{g}_1(x, v) &=& (a - b\,v)x, \end{array}\right\} \tag{39}$$

where $\boldsymbol{x} = x \in \mathbb{R}$ is the state variable of the extended memristor, $\hat{G}(\boldsymbol{x},\ v) = \hat{G}(x,\ v)$, and $\tilde{\boldsymbol{g}}(\boldsymbol{x},\ v) = \tilde{g}_1(x,\ v)$. Then Eq. (2) can be recast into Eq. (38).

In this case, the dynamics of the two-dimensional autonomous CNN in Fig. 2 is described by

$$\left.\begin{array}{rcl} \dfrac{dv_{i,j}}{dt} &=& -(c\,x_{i,j} - d)\,v_{i,j} + i_{i,j}, \\ \dfrac{dx_{i,j}}{dt} &=& (a - b\,v_{i,j} + v_{i,j})\,x_{i,j}, \\ \dfrac{d\varphi_{i,j}}{dt} &=& v_{i,j}, \end{array}\right\} \tag{40}$$

where $i = 1, 2, \cdots, N$, $j = 1, 2, \cdots, M$, and the four state variables of the CNN cell $n_{i,j}$ are explained as follow:

- $v_{i,j}$ is the voltage across the CNN cell, that is, the voltage across the capacitor C in the CNN cell.
- $i_{i,j}$ is the current though the CNN cell.
- $x_{i,j}$ is the state variable of the voltage-controlled *extended* memristor (see Eq. (1)).
- $\varphi_{i,j}$ is the flux of the capacitor C.

The current $i_{i,j}$ in Eq. (40) is given by

$$\begin{aligned} i_{i,j} &= W_g(\varphi_{i-1,j}-\varphi_{i,j})(v_{i-1,j}-v_{i,j}) - W_g(\varphi_{i,j}-\varphi_{i+1,j})(v_{i,j}-v_{i+1,j}) \\ &\quad + W_g(\varphi_{i,j-1}-\varphi_{i,j})(v_{i,j-1}-v_{i,j}) - W_g(\varphi_{i,j}-\varphi_{i,j+1})(v_{i,j}-v_{i,j+1}), \end{aligned} \tag{41}$$

where $W_g(\varphi_g)$ denotes the small-signal memductance of the voltage-controlled *ideal* memristors consisting the grid. The terminal current i_g and voltage v_g of the above memristors are given by

$$i_g = W_g(\varphi_g)\, v_g, \tag{42}$$

where φ_g is the flux of the ideal memristor, which satisfies $\dfrac{d\varphi_g}{dt} = v_g$ and $\varphi_g(0) = 0$. Assume that $W_g(\varphi_g)$ is given by

$$\left.\begin{aligned} W_g(\varphi_g) &= \mathfrak{s}\big[\,|\,\varphi_g\,| - 0.5\big] - \mathfrak{s}\big[\,|\,\varphi_g\,| - 3\,\big] \\ &= \left\{ \begin{array}{lll} 0 & \text{for} & |\varphi_g| < 0.5, \\ 1 & \text{for} & 0.5 \le |\varphi_g| < 3, \\ 0 & \text{for} & |\varphi_g| \ge 3. \end{array} \right\} \end{aligned}\right. \tag{43}$$

Then the ideal memristors consisting the grid are *passive*, since $W_g(\varphi_g) \ge 0$ and the instantaneous power $p(t)$ satisfies

$$p(t) = i_g(t)\, v_g(t) = W_g(\varphi_g(t))\, v_g(t)^2 \ge 0. \tag{44}$$

Note that when $|\,\varphi_g\,|$ is greater than 3 or less than 0.5, the memductance $W_g(\varphi_g)$ becomes *zero*, and the terminal current i_g does not flow into the memristor.

We show the two-dimensional nonlinear waves for $v_{i,j}$ in Fig. 11. The initial conditions $v^*_{i,j}(0)$ and $x^*_{i,j}(0)$ are equal to a black & white image or a gray-scale image in Fig. 6, where $v^*_{i,j}(0) = v_{i,j}(0) - 1.1$ and $x^*_{i,j}(0) = x_{i,j}(0) - 1.1$,[10] and we set $\varphi_{i,j}(0) = 0$. The boundary condition is given by Eq. (12). Observe that the four nonlinear waves in the autonomous Lotka-Volterra CNN (40) are completely different, that is, the nonlinear waves depend greatly on the initial conditions. It is partially thought to be caused by the fact that the Lotka-Volterra equations can be recast into the Hamilton's equations, which have *integral invariant* (see [2] for more details).

In this CNN, we have to use the *passive* memristor grid, since an *overflow* occurs in the numerical integration process when they are *locally active*. For example, assume that $W_g(\varphi_g)$ is given by

$$\left.\begin{aligned} W_g(\varphi_g) &= -1.5\,\mathfrak{s}\big[\,|\,\varphi_g\,| - 0.5\big] + 3\,\mathfrak{s}\big[\,|\,\varphi_g\,| - 7\,\big] \\ &= \left\{ \begin{array}{lll} 0 & \text{for} & |\varphi_g| < 0.5, \\ -1.5 & \text{for} & 0.5 \le |\varphi_g| < 7, \\ 1.5 & \text{for} & |\varphi_g| \ge 7. \end{array} \right\} \end{aligned}\right. \tag{45}$$

Then the ideal memristors consisting the grid become *locally* active, since the instantaneous power $p(t)$ satisfies

$$p(t) = i_g(t)\, v_g(t) = W_g(\varphi_g(t))\, v_g(t)^2 = -1.5\, v_g(t)^2 < 0, \tag{46}$$

for $0.5 < |\varphi_g(t)| < 7$ and $v_g(t) \neq 0$.

We show the two-dimensional nonlinear waves for the autonomous Lotka-Volterra CNN (40) in Fig. 13. Here, the initial condition and the boundary condition are the same as those for Eq. (43). Note that we could not obtain the nonlinear wave for $t = 14000$, since an *overflow* occurred in the numerical integration process. Here the step size h of the Euler method is set to 0.002. The initial conditions $v^*_{i,j}(0)$ and $x^*_{i,j}(0)$ are given by the image in Fig. 13 (1), where $v^*_{i,j}(0) = v_{i,j}(0) - 1.1$ and $x^*_{i,j}(0) = x_{i,j}(0) - 1.1$

[10] In order to avoid an overflow in the numerical simulations, we shifted the initial conditions.

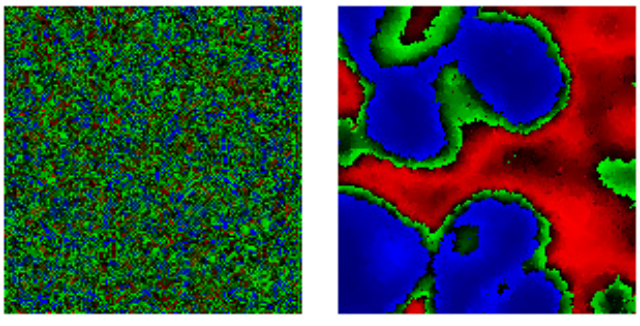

(a) $t = 6000$ (b) $t = 6000$

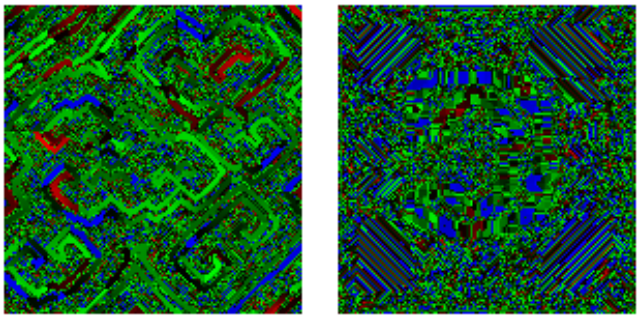

(c) $t = 6000$ (d) $t = 6000$

Figure 11: Two-dimensional nonlinear waves in the autonomous Lotka-Volterra CNN (40). These figures are not static, but dynamic (always changing) images at the instant of $t = 6000$. Observe that the four nonlinear waves are completely different, that is, the nonlinear waves depend greatly on the initial conditions. (a) The initial condition $v^*_{i,j}(0)$ is given by the upside-down text image in Fig. 6(1). (b) The initial condition $v^*_{i,j}(0)$ is given by the random noise image in Fig. 6(2). (c) The initial condition $v^*_{i,j}(0)$ is given by the gray-scale spiral image in Fig. 12(3). (d) The initial condition $v^*_{i,j}(0)$ is given by the flipped image of C in Fig. 12(4). Here, $v^*_{i,j}(0)$ is defined by $v^*_{i,j}(0) = v_{i,j}(0) - 1.1$. The step size h of the Euler method is all set to 0.002.

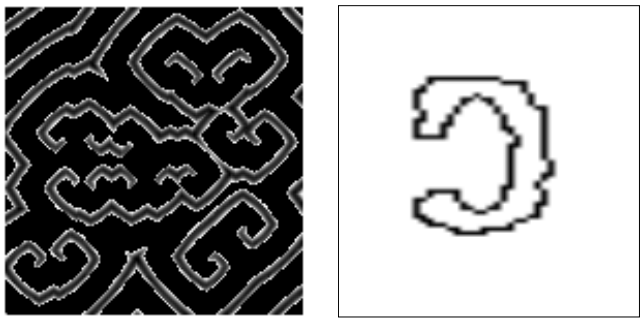

(3) (4)

Figure 12: Additional images for the initial condition $v_{i,j}(0)$. (3) a gray-scale spiral image. (4) a flipped image of C. They are both 145×150 pixels in size.

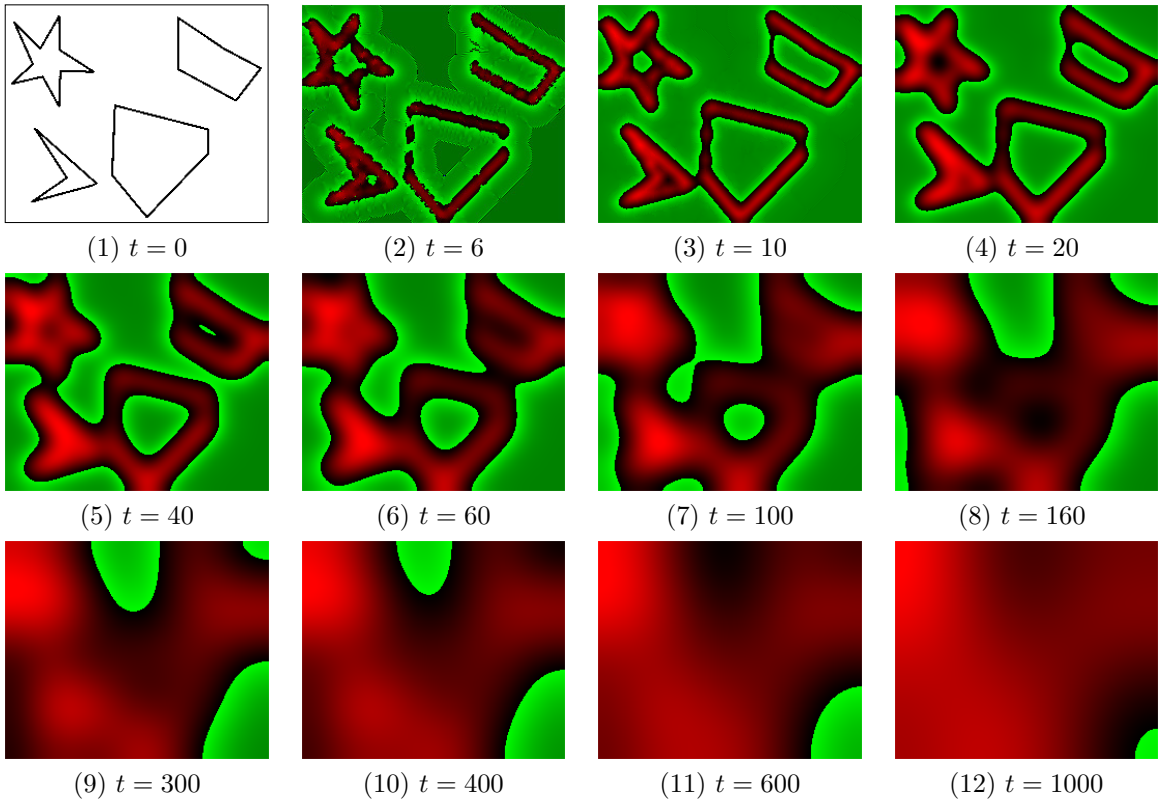

(1) $t = 0$ (2) $t = 6$ (3) $t = 10$ (4) $t = 20$

(5) $t = 40$ (6) $t = 60$ (7) $t = 100$ (8) $t = 160$

(9) $t = 300$ (10) $t = 400$ (11) $t = 600$ (12) $t = 1000$

Figure 13: Two-dimensional nonlinear waves in the autonomous Lotka-Volterra CNN (40). In this case, the grid consists of *locally active* memristors, whose memductance is given by Eq. (45). Initial condition $v^*_{i,j}(0)$ is given by the image in Fig. 13 (1) (255×211 pixels in size), where $v^*_{i,j}(0)$ is defined by $v^*_{i,j}(0) = v_{i,j}(0) - 1.1$. The step size h of the Euler method is set to 0.002. We could not obtain the nonlinear wave for $t = 14000$, since an *overflow* occurred in the numerical integration process.

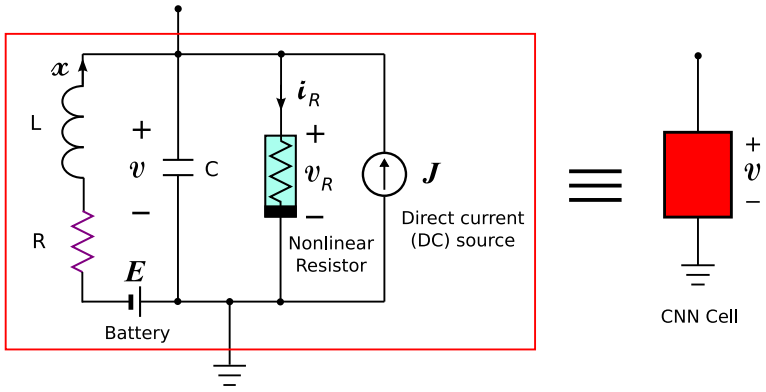

Figure 14: Circuit model for the FitzHugh-Nagumo equations (47). This circuit contains six circuit elements: a linear capacitor C, a linear inductor L, a linear resistor R, a direct current (DC) source J, a Battery E, and a nonlinear resistor, whose $v-i$ characteristic is given by $i_R = f(v_R) = \frac{{v_R}^3}{3} - v_R$. The circuit parameters are given by $C = \frac{1}{5}$, $L = 1$, $R_1 = 0.8$, $E = 0.7$, and $J = 0.5$.

3.5 Autonomous FitzHugh-Nagumo CNN

Consider the FitzHugh-Nagumo equations defined by (see [10] for more details)

$$\left.\begin{aligned} \frac{dv}{dt} &= 5\left(x - \frac{v^3}{3} - v + J\right), \\ \frac{dx}{dt} &= -v - 0.7 - 0.8x, \end{aligned}\right\} \tag{47}$$

where J denotes a *constant* current source. Equation (47) can be realized by the circuit in Fig. 14. Its dynamics is given by

$$\left.\begin{aligned} C\frac{dv}{dt} &= x - f(v) + J = x - \frac{v^3}{3} + v + J, \\ L\frac{dx}{dt} &= -v - E - Rx, \end{aligned}\right\} \tag{48}$$

where v and x respectively denote the voltage across the capacitor C and the current through the inductor L, and the $v-i$ characteristic of the nonlinear resistor is given by

$$i_R = f(v_R) \stackrel{\triangle}{=} \frac{{v_R}^3}{3} - v_R, \tag{49}$$

where $v = v_R$. The parameters in Eq. (48) satisfy

$$C = \frac{1}{5},\ L = 1,\ R = 0.8,\ E = 0.7,\ J = 0.5. \tag{50}$$

In this case, the dynamics of the two-dimensional autonomous CNN in Fig. 2 is described by

$$\left.\begin{array}{rcll} \dfrac{dv_{i,j}}{dt} & = & \dfrac{1}{C}\Big(x_{i,j} - f(v_{i,j}) + J + i_{i,j}\Big) & = & 5\left(x_{i,j} - \dfrac{{v_{i,j}}^3}{3} + v_{i,j} + 0.5 + i_{i,j}\right), \\ \dfrac{dx_{i,j}}{dt} & = & -v_{i,j} - E - Rx_{i,j} & = & -v_{i,j} - 0.7 - 0.8x_{i,j}, \\ \dfrac{d\varphi_{i,j}}{dt} & = & v_{i,j}, & & \end{array}\right\} \tag{51}$$

where $i = 1, 2, \cdots, N$, $j = 1, 2, \cdots, M$, the nonlinear function $f(v_{i,j})$ is given by

$$f(v_{i,j}) = \frac{{v_{i,j}}^3}{3} - v_{i,j}, \tag{52}$$

and the four state variables of the CNN cell $n_{i,j}$ are explained as follow:

- $v_{i,j}$ is the voltage across the CNN cell, that is, the voltage across the capacitor C in the CNN cell.
- $i_{i,j}$ is the current though the CNN cell.
- $x_{i,j}$ is the current through the inductor L in the CNN cell.
- $\varphi_{i,j}$ is the flux of the capacitor C in the CNN cell.

The current $i_{i,j}$ in Eq. (51) is given by

$$\begin{array}{rcl} i_{i,j} & = & W_g(\varphi_{i-1,j} - \varphi_{i,j})(v_{i-1,j} - v_{i,j}) - W_g(\varphi_{i,j} - \varphi_{i+1,j})(v_{i,j} - v_{i+1,j}) \\ & & +W_g(\varphi_{i,j-1} - \varphi_{i,j})(v_{i,j-1} - v_{i,j}) - W_g(\varphi_{i,j} - \varphi_{i,j+1})(v_{i,j} - v_{i,j+1}), \end{array} \tag{53}$$

where $W_g(\varphi_g)$ denotes the small-signal memductance of the voltage-controlled *ideal* memristors consisting the grid. The terminal current i_g and voltage v_g of the above memristors are given by

$$i_g = W_g(\varphi_g)\, v_g, \tag{54}$$

where φ_g is the flux of the ideal memristor, which satisfies $\dfrac{d\varphi_g}{dt} = v_g$ and $\varphi_g(0) = 0$. Assume that $W_g(\varphi_g)$ is given by

$$\left.\begin{array}{rcl} W_g(\varphi_g) & = & -\mathfrak{s}\big[\,|\,\varphi_g\,| - 0.5\,\big] + 2\,\mathfrak{s}\big[\,|\,\varphi_g\,| - 2\,\big] \\ & = & \left\{\begin{array}{cc} 0 \quad \text{for} & |\varphi_g| < 0.5, \\ -1 \quad \text{for} & 0.5 \le |\varphi_g| < 2, \\ 1 \quad \text{for} & |\varphi_g| \ge 2. \end{array}\right. \end{array}\right\} \tag{55}$$

Then the ideal memristors consisting the grid are *locally active*, since the instantaneous power $p(t)$ satisfies

$$p(t) = i_g(t)\, v_g(t) = W_g(\varphi_g(t))\, v_g(t)^2 = -v_g(t)^2 < 0, \tag{56}$$

for $0.5 < |\varphi_g(t)| < 2$ and $v_g(t) \neq 0$.

We show the two-dimensional nonlinear waves for $v_{i,j}$ in Fig. 15. Observe that the nonlinear waves of the two-dimensional autonomous FitzHugh-Nagumo CNN (51) can exhibit complex nonlinear waves. Here, the initial condition $v_{i,j}(0)$ is equal to a black & white image or a gray-scale image in Fig. 6, and we set $x_{i,j}(0) = \varphi_{i,j}(0) = 0$. The boundary condition is given by Eq. (12).

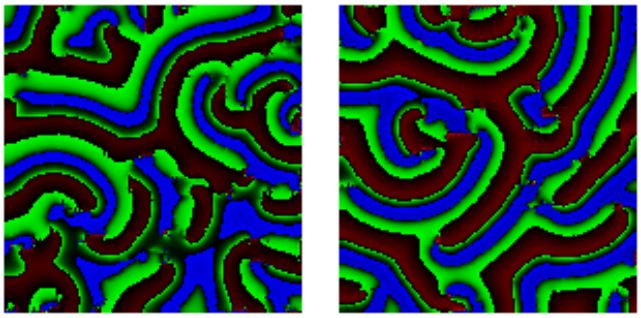

(a) $t = 10000$ (b) $t = 10000$

Figure 15: Two-dimensional nonlinear waves in the autonomous FitzHugh-Nagumo CNN (51). These figures are not static, but dynamic (always changing) images at the instant of $t = 10000$. (a) The initial condition $v_{i,j}(0)$ is given by the upside-down text image in Fig. 6(1). (b) The initial condition $v_{i,j}(0)$ is given by the random noise image in Fig. 6(2). The step size h of the Euler method is both set to 0.02.

3.6 Autonomous Van der Pol CNN

The FitzHugh-Nagumo equations contains the Van der Pol oscillator as a special case, that is, we can obtain the Van der Pol oscillator if we set $C = L = 1$ and $J = E = R = 0$ for Eq. (48).

In this case, the dynamics of the two-dimensional autonomous Van der Pol CNN is given by

$$\left.\begin{aligned} \frac{dv_{i,j}}{dt} &= x_{i,j} - f(v_{i,j}) + i_{i,j} = x_{i,j} - \frac{{v_{i,j}}^3}{3} + v_{i,j} + i_{i,j}, \\ \frac{dx_{i,j}}{dt} &= -v_{i,j}, \\ \frac{d\varphi_{i,j}}{dt} &= v_{i,j}, \end{aligned}\right\} \tag{57}$$

where $i = 1, 2, \cdots, N$, $j = 1, 2, \cdots, M$, the nonlinear function $f(v_{i,j})$ is given by

$$f(v_{i,j}) = \frac{{v_{i,j}}^3}{3} - v_{i,j}, \tag{58}$$

and the four state variables of the CNN cell $n_{i,j}$ are explained as follow:

- $v_{i,j}$ is the voltage across the CNN cell, that is, the voltage across the capacitor C in the CNN cell.
- $i_{i,j}$ is the current though the CNN cell.
- $x_{i,j}$ is the current through the inductor L in the CNN cell.
- $\varphi_{i,j}$ is the flux of the capacitor C in the CNN cell.

The current $i_{i,j}$ in Eq. (57) is given by is given by

$$\begin{aligned} i_{i,j} \;=\; & W_g(\varphi_{i-1,j} - \varphi_{i,j})(v_{i-1,j} - v_{i,j}) - W_g(\varphi_{i,j} - \varphi_{i+1,j})(v_{i,j} - v_{i+1,j}) \\ & + W_g(\varphi_{i,j-1} - \varphi_{i,j})(v_{i,j-1} - v_{i,j}) - W_g(\varphi_{i,j} - \varphi_{i,j+1})(v_{i,j} - v_{i,j+1}), \end{aligned} \tag{59}$$

where $W_g(\varphi_g)$ denotes the small-signal memductance of the voltage-controlled *ideal* memristors consisting the grid. The terminal current i_g and voltage v_g of the above memristors are given by

$$i_g = W_g(\varphi_g)\, v_g, \tag{60}$$

where φ_g is the flux of the ideal memristor, which satisfies $\dfrac{d\varphi_g}{dt} = v_g$ and $\varphi_g(0) = 0$. Assume that $W_g(\varphi_g)$

is given by

$$\left.\begin{aligned} W_g(\varphi_g) &= \mathfrak{s}\big[\,|\,\varphi_g\,|-0.5\,\big]+2\,\mathfrak{s}\big[\,|\,\varphi_g\,|-7\,\big] \\ &= \begin{cases} 0 & \text{for} \quad |\varphi_g|<0.5, \\ 1 & \text{for} \quad 0.5\le|\varphi_g|<7, \\ 3 & \text{for} \quad |\varphi_g|\ge 7. \end{cases} \end{aligned}\right\} \tag{61}$$

Then the ideal memristors consisting the grid are *passive*, since the instantaneous power $p(t)$ satisfies

$$p(t)=i_g(t)\,v_g(t)=W_g(\varphi_g(t))\,v_g(t)^2\ge 0. \tag{62}$$

We show the two-dimensional nonlinear waves for $v_{i,j}$ in Fig. 16. The autonomous Van der Pol CNN (57) can exhibit complex nonlinear waves. Here, the initial condition $v_{i,j}(0)$ is equal to a black & white image or a gray-scale image in Fig. 6, and we set $x_{i,j}(0)=\varphi_{i,j}(0)=0$. The boundary condition is given by Eq. (12).

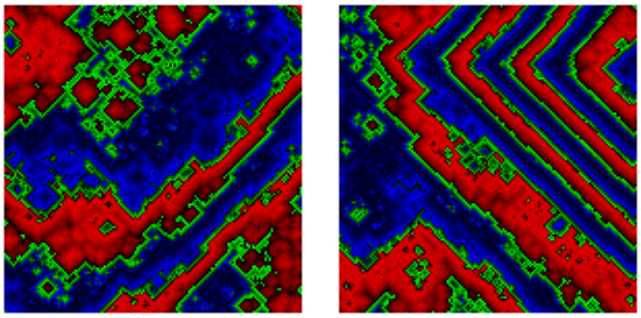

(a) $t=80000$ (b) $t=80000$

Figure 16: Two-dimensional nonlinear waves in the autonomous Van der Pol CNN (57). These figures are not static, but dynamic (always changing) images at the instant of $t=80000$. The $v-i$ characteristic of the nonlinear resistor is given by $i_R=f(v_R)=\dfrac{{v_R}^3}{3}-v_R$. (a) The initial condition $v_{i,j}(0)$ is given by the upside-down text image in Fig. 6(1). (b) The initial condition $v_{i,j}(0)$ is given by the random noise image in Fig. 6(2). The step size h of the Euler method is both set to 0.2.

We next show that the two-dimensional autonomous Van der Pol type CNN (57) can exhibit interesting wave patterns by changing the $v-i$ characteristic of the nonlinear resistor in Fig. 14, that is, by changing the nonlinear function $f(v_R)$.

Case A. Assume that $v-i$ characteristic of the nonlinear resistor in Fig. 14 is given by

$$i_R=f(v_R)=v_R+1.5|v_R-1|-1.5, \tag{63}$$

and assume that the initial condition and the boundary condition are same as those for Eq. (57). Then, we obtain the nonlinear waves in Fig. 17.

Case B. Assume that $v-i$ characteristic of the nonlinear resistor in Fig. 14 is given by

$$i_R=f(v_R)=0.01{v_R}^3+0.25{v_R}^2-0.25v_R, \tag{64}$$

and assume that the initial condition and the boundary condition are same as those for Eq. (57). Then, we obtain the nonlinear waves in Fig. 18. Furthermore, if we choose a different value for the step size h of the Euler method, the autonomous Van der Pol type CNN (57) exhibit different nonlinear waves as shown in Fig. 19.

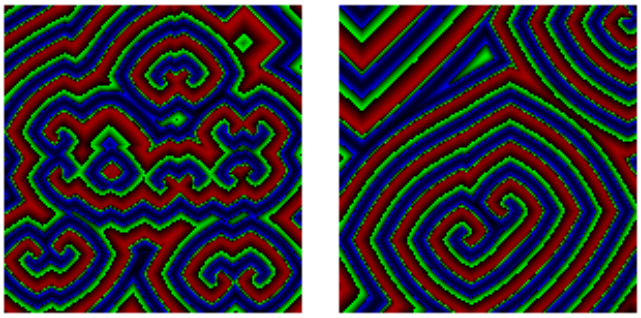

(a) $t = 2000$ (b) $t = 2000$

Figure 17: Two-dimensional nonlinear waves in the autonomous Van der Pol type CNN (57). These figures are not static, but dynamic (always changing) images at the instant of $t = 2000$. The $v - i$ characteristic of the nonlinear resistor is given by $i_R = f(v_R) = v_R + 1.5|v_R - 1| - 1.5$. (a) The initial condition $v_{i,j}(0)$ is given by the upside-down text image in Fig. 6(1). (b) The initial condition $v_{i,j}(0)$ is given by the random noise image in Fig. 6(2). The step size h of the Euler method is both set to 0.01.

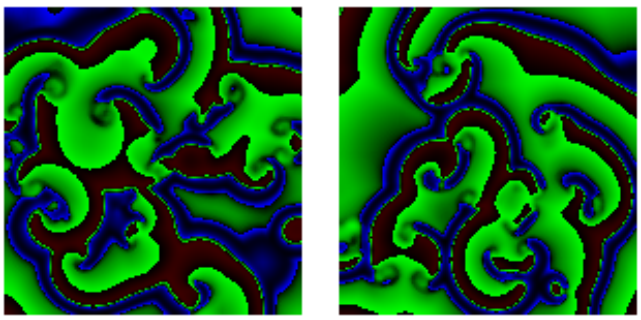

(a) $t = 3000$ (b) $t = 3000$

Figure 18: Two-dimensional nonlinear waves in the autonomous Van der Pol type CNN (57). These figures are not static, but dynamic (always changing) images at the instant of $t = 3000$. The $v - i$ characteristic of the nonlinear resistor is given by $i_R = f(v_R) = 0.01{v_R}^3 + 0.25{v_R}^2 - 0.25v_R$. (a) The initial condition $v_{i,j}(0)$ is given by the upside-down text image in Fig. 6(1). (b) The initial condition $v_{i,j}(0)$ is given by the random noise image in Fig. 6(2). The step size h of the Euler method is both set to 0.03.

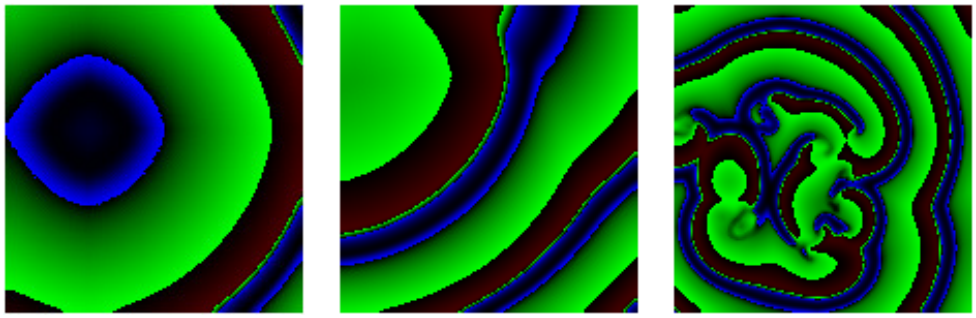

(a) $h = 0.1$ (b) $h = 0.06$ (b) $h = 0.03$

Figure 19: Nonlinear waves in the autonomous Van der Pol type CNN (57) for $h = 0.1$, $h = 0.06$, and $h = 0.03$ at $t = 1200$. Here h denotes the step size of the Euler method. Observe that Eq. (57) exhibits different nonlinear waves, if we choose a different value for the step size h. The $v - i$ characteristic of the nonlinear resistor is given by $i_R = f(v_R) = 0.01{v_R}^3 + 0.25{v_R}^2 - 0.25v_R$. The initial condition $v_{i,j}(0)$ is given by the random noise image in Fig. 6(2).

3.7 Autonomous Chua circuit CNN

The dynamics of the Chua circuit [11, 12] is defined by

$$\left.\begin{aligned} \frac{dv}{dt} &= \alpha\big(x - v - f(v)\big), \\ \frac{dx}{dt} &= v - x + y, \\ \frac{dy}{dt} &= -\beta x, \end{aligned}\right\} \tag{65}$$

where $\alpha = 10$, $\beta = 14$, and $f(v)$ is a scalar function of a single variable v defined by

$$f(v) = \frac{1}{16}v^3 - \frac{7}{6}v. \tag{66}$$

Equation (65) can be realized by the circuit in Fig. 20 (see [4] and [11]). Its dynamics is given by

$$\left.\begin{aligned} C_1\frac{dv}{dt} &= \frac{x - v}{R} - f(v), \\ C_2\frac{dx}{dt} &= y - \frac{x - v}{R}, \\ L\frac{dy}{dt} &= -x, \end{aligned}\right\} \tag{67}$$

where the symbols v, x, and y denote the voltage across the capacitor C_1, the voltage across the capacitor C_2, and the current through the inductor L, respectively. These parameters satisfy

$$C_1 = \frac{1}{\alpha} = \frac{1}{10},\ C_2 = 1,\ L = \frac{1}{\beta} = \frac{1}{14},\ R = 1, \tag{68}$$

and $v - i$ characteristic of the nonlinear resistor is given by

$$i_R = f(v_R) = \frac{1}{16}{v_R}^3 - \frac{7}{6}v_R. \tag{69}$$

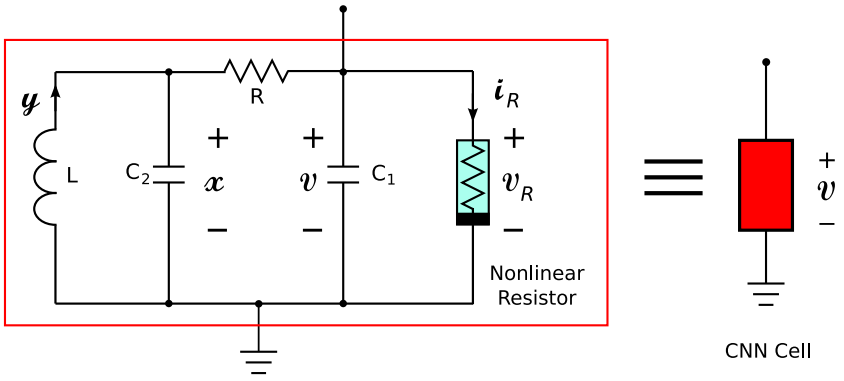

Figure 20: Chua circuit, which contains five circuit elements: two linear capacitors C_1 and C_2, one linear inductor L, one linear resistor R, and one *nonlinear* resistor. The $v-i$ characteristic of the nonlinear resistor is given by $i_R = f(v_R) = \frac{1}{16}{v_R}^3 - \frac{7}{6}v_R$. The circuit parameters are given by $C_1 = \frac{1}{10}$, $C_2 = 1$, $L = \frac{1}{14}$, and $R = 1$.

In this case, the dynamics of the two-dimensional autonomous CNN in Fig. 2 is described by

$$\left.\begin{array}{rcl} \dfrac{dv_{i,j}}{dt} &=& \alpha\Big(x_{i,j} - v_{i,j} - f(v_{i,j}) + i_{i,j}\Big), \\ \dfrac{dx_{i,j}}{dt} &=& v_{i,j} - x_{i,j} + y_{i,j}, \\ \dfrac{dy_{i,j}}{dt} &=& -\beta x_{i,j}, \\ \dfrac{d\varphi_{i,j}}{dt} &=& v_{i,j}, \end{array}\right\} \tag{70}$$

where $i = 1, 2, \cdots, N$, $j = 1, 2, \cdots, M$, and the five state variables of the CNN cell $n_{i,j}$ are explained as follow:

- $v_{i,j}$ is the voltage across the CNN cell, that is, the voltage across the capacitor C_1 in the CNN cell.
- $i_{i,j}$ is the current though the CNN cell.
- $x_{i,j}$ is the voltage across the capacitor C_2 in the CNN cell.
- $y_{i,j}$ is the current though the inductor L in the CNN cell.
- $\varphi_{i,j}$ is the flux of the capacitor C_1 in the CNN cell.

The current $i_{i,j}$ in Eq. (70) is given by

$$\begin{array}{rcl} i_{i,j} &=& W_g(\varphi_{i-1,j} - \varphi_{i,j})(v_{i-1,j} - v_{i,j}) - W_g(\varphi_{i,j} - \varphi_{i+1,j})(v_{i,j} - v_{i+1,j}) \\ && + W_g(\varphi_{i,j-1} - \varphi_{i,j})(v_{i,j-1} - v_{i,j}) - W_g(\varphi_{i,j} - \varphi_{i,j+1})(v_{i,j} - v_{i,j+1}), \end{array} \tag{71}$$

where $W_g(\varphi_g)$ denotes the small-signal memductance of the voltage-controlled *ideal* memristors consisting the grid. The terminal current i_g and voltage v_g of the above memristors are given by

$$i_g = W_g(\varphi_g)\, v_g, \tag{72}$$

where φ_g is the flux of the ideal memristor, which satisfies $\dfrac{d\varphi_g}{dt} = v_g$ and $\varphi_g(0) = 0$. Assume that $W_g(\varphi_g)$ is given by

$$\left.\begin{array}{rcl} W_g(\varphi_g) &=& -\mathfrak{s}\big[\,|\,\varphi_g\,| - 0.5\,\big] + 4\,\mathfrak{s}\big[\,|\,\varphi_g\,| - 7\,\big] \\ &=& \left\{\begin{array}{ccc} 0 & \text{for} & |\varphi_g| < 0.5, \\ -1 & \text{for} & 0.5 \le |\varphi_g| < 7, \\ 3 & \text{for} & |\varphi_g| \ge 7. \end{array}\right. \end{array}\right\} \tag{73}$$

Then the ideal memristors consisting the grid are *locally active*, since the instantaneous power $p(t)$ satisfies

$$p(t) = i_g(t)\, v_g(t) = W_g(\varphi_g(t))\, v_g(t)^2 = -v_g(t)^2 < 0, \tag{74}$$

for $0.5 < |\varphi_g(t)| < 7$ and $v_g(t) \neq 0$.

We show the two-dimensional nonlinear waves for $v_{i,j}$ in Fig. 21. Observe that the autonomous Chua circuit CNN (70) can exhibit complex nonlinear waves. The initial conditions $v^*_{i,j}(0)$, $x^*_{i,j}(0)$, and $y^*_{i,j}(0)$ are equal to a black & white image or a gray-scale image in Fig. 6, and we set $\varphi_{i,j}(0) = 0$, where $v_{i,j}(0) = 1.1\, v^*_{i,j}(0)$, $x_{i,j}(0) = 1.1\, x^*_{i,j}(0)$, and $y_{i,j}(0) = 1.1\, y^*_{i,j}(0)$.[11] The boundary condition is given by Eq. (12).

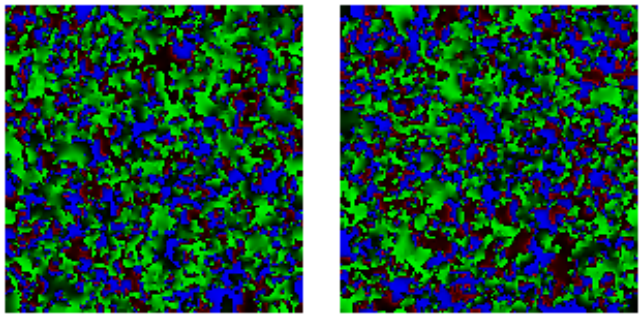

(a) $t = 1000$ (b) $t = 1000$

Figure 21: Two-dimensional nonlinear waves in the autonomous Chua circuit CNN (70). These figures are not static, but dynamic (always changing) images at the instant of $t = 1000$. (a) The initial condition $v^*_{i,j}(0)$ is given by the upside-down text image in Fig. 6(1). (b) The initial condition $v^*_{i,j}(0)$ is given by the random noise image in Fig. 6(2). We scaled the initial conditions by multiplying them 1.1, in order to avoid an overflow in the numerical simulations. That is, $v_{i,j}(0) = 1.1\, v^*_{i,j}(0)$. The step size h of the Euler method is both set to 0.005.

4 Conclusion

We have shown that the two-dimensional autonomous CNNs coupled by memristors can exhibit interesting and complex nonlinear waves. Furthermore, we have shown that some autonomous CNN can exhibit various kinds of nonlinear waves by changing the initial conditions, or by changing the characteristic curve of the nonlinear resistor. It suggests that neural networks are capable of more complex responses by using the memristors. In this paper, we used the Euler method for solving the autonomous CNN equations. In order to get more accurate results, we may need high accuracy numerical methods, for example, the Runge-Kutta method.

[11] We used the scaled initial conditions in order to avoid an overflow in the numerical simulations.

References

[1] Itoh, M.(2019) Some Interesting Features of Memristor CNN, arXiv:1902.05167 [cs.NE].

[2] Itoh, M.(2019b) Memristor Circuit Equations with Periodic Forcing, viXra:1902.0345 [Category: Mathematical Physics].

[3] Itoh, M. and Chua, L. (2017) Chaotic oscillation via edge of chaos criteria, *Int. J. Bifurcation and Chaos* **27**(11), 1730035-1–79.

[4] Chua L.O., Hasler M., Moschytz G.S., and Neirynsk J. (1995) Autonomous Cellular Neural Networks: A Unified Paradigm for Pattern Formation and Active Wave Propagation, *IEEE Trans. CAS-I*, **42**(10), 559-577.

[5] Chua, L.O. (1998) *CNN: A Paradigm for Complexity* (World Scientific, Singapore).

[6] Chua, L.O. and Roska, T. (2002) *Cellular neural networks and visual computing* (Cambridge University Press, Cambridge), 2002.

[7] Van Valkenburg, M.E. (1964) *Network Analysis* (Prentice-Hall, Englewood Cliffs, N.J.).

[8] Chua, L. (2015) Everything You Wish to Know About Memristors But Are Afraid to Ask, *Radioengineering* **24**(2), 319-368.

[9] Asai T. (2014) Reaction-Diffusion Media with Excitable Oregonators Coupled by Memristors, in: Adamatzky A. and Chua L. (eds.) Memristor Networks (Springer, Switzerland).

[10] Izhikevich, E.M. and FitzHugh, R. (2006) "FitzHugh-Nagumo Model," *Scholarpedia* **1**(9), 1349.

[11] Madan, R.N. (1993) *Chua's Circuit: A Paradigm for Chaos* (World Scientific, Singapore).

[12] Hirsch, M.W., Smale, S., and Devaney, R.L. (2003) *Differential Equations, Dynamical Systems, and an Introduction to Chaos, Second Edition* (Elsevier Academic Press, Amsterdam).